

Near-neighbor defect contribution to the hyperfine field of Fe in Fe

Ch. Stenzel

*Physics Department, State University of New York at Stony Brook, Stony Brook, New York 11794
and Bereich Kern- und Strahlenphysik, Hahn-Meitner-Institut Berlin GmbH, Berlin, Germany
and Fachbereich Physik, Freie Universität Berlin, D-1000 Berlin 39, Germany*

J. Das, T. Lauritsen, J. Schecker, and G. D. Sprouse

Physics Department, State University of New York at Stony Brook, Stony Brook, New York 11794

H.-E. Mahnke

*Physics Department, State University of New York at Stony Brook, Stony Brook, New York 11794
and Bereich Kern- und Strahlenphysik, Hahn-Meitner-Institut Berlin GmbH, Berlin, Germany
and Fachbereich Physik, Freie Universität Berlin, D-1000 Berlin 39, Germany*

(Received 20 July 1988)

The magnetic hyperfine fields at isomeric ^{54}Fe nuclei have been measured in Fe and Ni at 85 and 295 K by observation of the spin precession time-differentially with high time resolution following recoil implantation. In iron at 85 K a unique defect structure has been detected by its well-resolved magnetic hyperfine field which differs considerably from the value for the substitutional site. This defect is tentatively assigned to be a monovacancy in the next-nearest neighborhood of the probe atom. The change of the hyperfine field by such a vacancy is similar to the change caused by adjacent impurity atoms in dilute Fe alloys.

Nuclear methods have become effective tools for studying point defects in metals on a microscopic scale. Point defects in the neighborhood of a nuclear probe have been identified by the change of the charge distribution around the probe atom. In cubic lattices the electric field gradient (efg) observed via hyperfine interaction with the nuclear quadrupole moment is different for each type of defect, while in noncubic lattices the inherent efg may be altered in characteristic ways by defects. With various microscopic methods such as Mössbauer spectroscopy, perturbed angular correlation, and positron annihilation many kinds of defects have been investigated in different metals over the last decade.¹⁻³

In ferromagnetic materials near-neighbor defects do not only change the charge distribution but also the spin distribution, which may result in different magnetic fields at the probe atom next to the defect. In total, a combined interaction, magnetic and electric, has to be expected. It would greatly help to understand the origin of the internal magnetic field to know the magnetic behavior of an iron probe in a well-defined altered iron environment. So far the defect's influence on the magnetic field was detected only at nonmagnetic impurity atoms in defect-impurity configurations (see Refs. 1 and 2): In the case of iron different magnetic fields have been observed for different defect configurations at the site of the impurity atoms Cs and Sn; in nickel unique configurations have been identified for the impurity atoms Cd and Sn. In both materials the defects are observed because of their trapping at an impurity atom. At the self-atom, however, no unique defect structure could be observed so far, although many attempts have been made especially by Mössbauer spectroscopy on ^{57}Fe in Fe.⁴⁻⁶

In the case of iron there exists a very favorable alterna-

tive to Mössbauer spectroscopy in ^{57}Fe . We have applied the high-resolution perturbed angular distribution⁷ (PAD) of the 10^+ isomer of ^{54}Fe to determine the characteristic change of the magnetic field due to a well-defined nearby defect. The larger nuclear g factor and the longer lifetime of the ^{54}Fe isomer [$T_{1/2} = 357$ ns, $g = 0.73$, $Q = 28$ fm² (Ref. 8)] yield a factor of 30 improvement in terms of resolving different magnetic fields as compared to the Mössbauer nucleus ^{57}Fe . The ^{54}Fe isomer is produced in a heavy-ion reaction, the excited probe nuclei recoil out of the target foil and can be deeply implanted into the host material. During the implantation the recoiling atoms produce correlated defects in the host lattice which may be observed nanoseconds after their production.

To take full advantage of the sensitivity of ^{54}Fe a high time resolution is necessary to resolve the fast modulation caused by the spin precession in the magnetic field at the nucleus. The experiment which we report here was done with a pulsed 40-MeV ^{12}C beam (repetition time was 1.3 μs) from the tandem-superconducting linear accelerator at Stony Brook to produce the isomeric ^{54}Fe in the $^{45}\text{Sc}(^{12}\text{C}, p, 2n)$ reaction. Using the linear accelerator modules not as a post accelerator but rather two single resonators as beam bunchers an overall time resolution of $\Delta t \approx 800$ ps was achieved when detecting the 3.4-MeV γ radiation from the decay of the isomer with BaF_2 scintillators of 3.8×2.5 -cm size. The iron sample, an annealed natural Fe foil of 99.998% purity (metallic impurities), had a thickness of 2.1 mg/cm² to allow the beam particles to go through but to stop all nuclei recoiling out of the 1-mg/cm² Sc foil. The beam was stopped in a Pb foil behind the Fe sample. The sample with the Sc foil on top was mounted on the cold plate of a Joule-Thomson cryotip to vary the temperature between 77 K and room tempera-

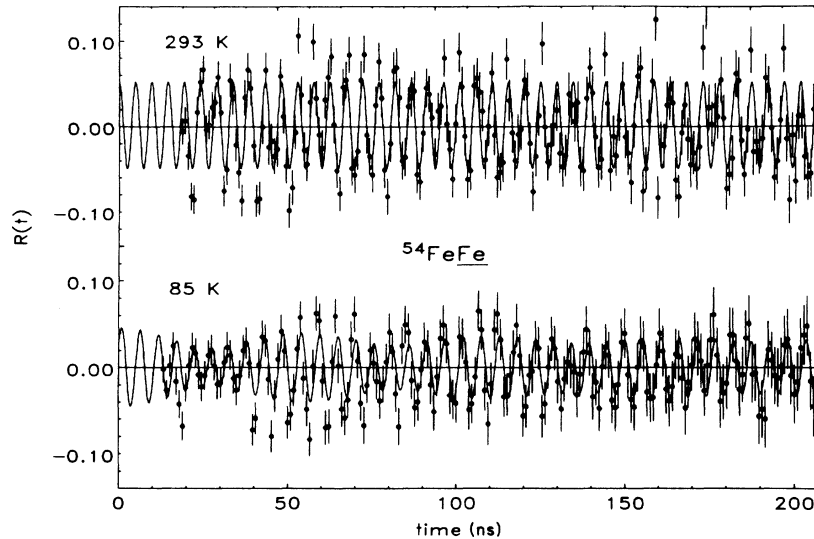


FIG. 1. Modulation spectra of ^{54}Fe in Fe at room temperature (top) and at 85 K (bottom).

ture, and it was magnetized with SmCo permanent magnets. The experiment was performed in the so-called “45° geometry”⁹ in which the plane of the iron foil (and the direction of the magnetizing field) is positioned in the detector plane to yield an angle of 45° with respect to the beam direction. In this arrangement the fundamental Larmor frequency is observed in PAD rather than a harmonic due to the symmetry of the angular distribution. From the measured time spectra in the detectors at the positions of 0° and 90° with respect to the beam, the intensity modulation is extracted in the usual way.

In both hosts, iron and nickel, we observed a single damped Larmor precession of the nuclear spins at room temperature corresponding to the interaction of the nuclear magnetic moment with the effective field at the nucleus. The amplitude of the modulation was slightly larger in the case of nickel as compared to iron. At 85 K the total amplitude of the modulation is reduced in both hosts. In nickel, again a single undamped precession frequency is found, shifted according to the temperature dependence of the bulk magnetization. In iron, however, the modulation spectrum showed a significant beat pattern due to a superposition of two cosinelike modulations of different intensities with slightly different frequencies. The more intense component showed the expected small frequency shift according to the temperature dependence of the magnetization. The less intense fraction is strongly damped and its frequency is reduced. Figure 1 shows the modulation spectra at the two different temperatures. The fitted curve to the low-temperature data assumes two fractions, f_1 and f_2 , with different frequencies, ν_1 and ν_2 . For the fraction f_2 a Lorentzian-like damping parameter was fitted as well. A better illustration of the two components is given by the Fourier transform of the modulation spectra as presented in Fig. 2, where the second component shows up as a small satellite at 168.5 MHz. The extracted parameters are summarized in Table I. The internal field values H_{int} were determined by using the

value for Fe in Fe at 298 K from Violet and Pipkorn¹⁰ as calibration for the nuclear g factor [$g = 0.730(1)$ in agreement with the previous determination⁸]. The values for the internal magnetic fields of iron in nickel are also in good agreement with a recent Mössbauer study.¹¹ The achieved accuracy of the present work is considerably

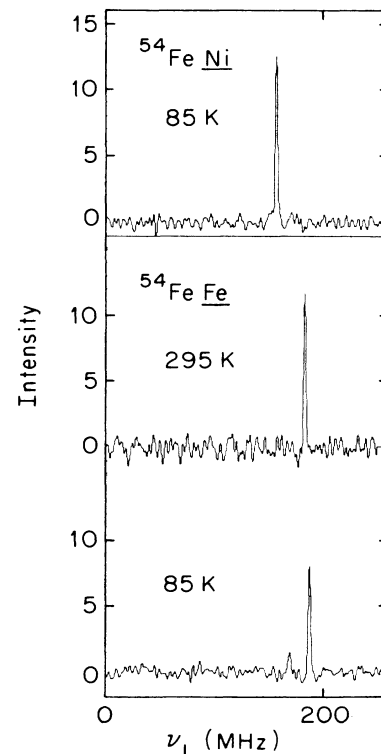


FIG. 2. Fourier transforms of the modulation spectra of ^{54}Fe in Fe and Ni at room temperature and 85 K. Intensity in arbitrary units.

TABLE I. Effective anisotropies A_{22} , fractions f_i , Larmor precession frequencies ν_i , and hyperfine magnetic fields $H_{\text{int}}(i)$ of the component i of ^{54}Fe in Fe and Ni with an external magnetizing field of 0.15(1) T. Exponential damping times $\tau_{\text{damp}}(i)$ of significant value were obtained only for the second component.

	$^{54}\text{FeFe}$		$^{54}\text{FeNi}$	
	85	300	85	300
T (K)	85	300	85	300
A_{22}	0.041(3)	0.070(3)	0.059(3)	0.085(4)
f_1	0.8(2)	1	1	1
ν_1 (MHz)	187.3(1)	183.05(15)	156.36(15)	146.95(10)
f_2	0.2(1)	0	0	0
$\tau_{\text{damp}}(2)$ (μs)	0.30(8)
ν_2 (MHz)	168.5(3)
$H_{\text{int}}(1)$ (T)	33.81(6)	33.04	28.25(6)	26.56(6)
$H_{\text{int}}(2)$ (T)	30.5(2)

higher, mainly due to the better sensitivity of the ^{54}Fe probe.

The overall agreement with the Mössbauer data clearly indicates that the modulation in nickel and the modulation of the major component in iron originate from ^{54}Fe substituted for a lattice atom. The satellite peak in iron at 85 K is then associated with a ^{54}Fe atom decorated with a well-defined defect. This defect structure is thermally healed out upon raising the temperature to room temperature. The annealing processes for simple point defects such as vacancies and interstitials in iron have been well studied with conventional and also with nuclear methods (see Ref. 3). The free migration of interstitials (step I_e in the one-interstitial model) sets in at temperatures higher than 120 K. Vacancies are mobile above 220 K. But these annealing steps were determined in experiments with annealing times of several minutes. The observed recovery temperatures in an in-beam PAD experiment, however, are considerably raised: The Larmor period sets the time window during which the annealing has to take place. This means that several nanoseconds rather than several minutes are characteristic for the annealing time. Assuming a simple Arrhenius-type temperature behavior for the jump frequency the annealing steps in a PAD experiment are shifted to temperatures about two to three times higher.¹²

It then follows that the observed disappearance of the satellite peak in iron is related to the migration of interstitial atoms. These defects are immobile at 85 K but are able to make enough jumps during the Larmor period at 300 K so that they could be regarded as freely migrating in this very short time range. Therefore three simple probe-defect configurations are possible: (i) the ^{54}Fe probe sits at a regular lattice site decorated with an interstitial-like defect, (ii) the probe is sitting at a regular lattice site with a vacancy next to it, and (iii) the nuclear probe itself is part of an interstitial-like defect. In all three cases the free migration of interstitial atoms would reduce the fraction of the respective configuration, not only in cases (i) and (iii), but also in case (ii) by annihilation of vacancies.^{13,14} Although no direct proof can be

presented configuration (ii) is the most likely one for the following reasons: The implantation of iron atoms into an iron host leads to a much higher probability for landing at a regular lattice site than for an impurity atom; therefore, configuration (iii) seems very unlikely. Furthermore, since the ^{54}Fe probe atom is a self-atom in the iron matrix, there is no trapping of defects or interstitial impurities such as O_2 , N_2 , and C by the probe atom itself. Instead, several studies of lattice damage by recoiling nuclei have shown that the probe atom is surrounded by a vacancy-rich zone, which itself is surrounded by a region of increased interstitial density. This picture is derived from the preferred Frenkel pair production at the end of the collision cascade.^{15,16} These arguments strongly favor the vacancylike configuration (ii) over the interstitial-like configuration (i) for the observed defect structure.

Our assignment is supported by a similar observation following the implantation of Cd probe nuclei into Pd metal. Bertschat *et al.* found in a similar PAD experiment that about 4% of the recoiling nuclei showed a modulation pattern due to the quadrupole interaction of the Cd probe with a vacancy in the next neighborhood; the defect structure was confirmed by neutron irradiation experiments.¹⁷ The fraction of nuclei which experiences the unique defect structure of a next-neighbor vacancy is close to that observed in the present experiment.

The fraction of probe atoms contributing to the measured modulation signal is reduced over the theoretically possible value. The maximum anisotropy found experimentally is $A_{22}=0.21(3)$ using other, nonmagnetic host materials.¹⁸ The observed anisotropy in iron, however, was found to be less than half of that value, even at room temperature. The reason for the reduced signal is not clear, especially since several mechanisms could have contributed. But it should be added that the observed fraction for the substitutional site in iron is in good agreement with a computer simulation for the implantation of Fe into Fe by Doran.¹⁴

In the nickel host, we have found no additional satellite peak and also no significant damping at liquid-nitrogen temperature. A possible explanation might be that because of the smaller size of the implanted iron ion the iron probe atoms are tending to repel vacancies. Then the fraction of probe atoms decorated with a vacancy is somewhat smaller compared to the iron case, becoming too low for our present detection efficiency.

Our assignment of the observed satellite peak in iron to a nearby vacancy can now be taken to compare its magnetic field with the magnetic behavior of Fe probes in dilute Fe alloys. Up to now no one has observed the direct influence of a point defect on the magnetic hyperfine field in pure iron or other pure systems. Instead, many Mössbauer and also NMR experiments have been performed to investigate that question using dilute alloys and a general trend has been found: The magnetic field at the site of the Fe probe is smaller than in pure α -Fe if the probe is surrounded with at least one nonmagnetic impurity in its near neighborhood. This has been measured in dilute nonordered FeX alloys ($X=\text{V}$, Ti, Al, and Si).^{19,20} The magnetic hyperfine field at the Fe site with an aluminum atom in the nearest-neighbor shell was measured to

be about 7% smaller than the field at the Fe site with no impurity atom nearby. For an aluminum atom in the further remote shells this reduction was somewhat less.

This behavior suggests that a vacancy should also behave as such a "magnetic hole." Indeed, the observed reduction in the hyperfine field is quite similar to the change found in the dilute iron alloys with nonmagnetic partners. In addition, Fe atoms in the (110) surface of Fe also experience a reduction in the magnetic field of similar size.²¹ Besides the changes in the arrangement of the surrounding atomic moments the charge distribution is also affected and an electric field gradient has to be expected. Indeed, the observed damping of the modulation of the second fraction can be interpreted as a quadrupole frequency⁸ of approximately $e^2qQ/h = 40(10)$ MHz for the ⁵⁴Fe probe which translates into an efg of $V_{zz} \approx 6 \times 10^{17}$

V/cm². While the efg on Fe in Fe-interstitial configurations in other bcc metals is considerably larger,²² the efg at a Fe (110) surface is of similar magnitude (see Ref. 21 after recalculation with the proper quadrupole moment⁸).

In summary, we have observed for the first time in the pure Fe system, the modification of the internal magnetic field by a nearby defect. The change in the internal magnetic field observed is similar to the change observed for Fe atoms next to nonmagnetic impurities and Fe atoms on the surface. Based on the implantation dynamics, the observed change is due to a vacancy adjacent to the Fe atom.

This work was in part supported by the National Science Foundation.

-
- ¹Th. Wichert, *Hyperfine Interact.* **15/16**, 335 (1983).
²R. Sielemann, *Mater. Sci. Forum* **15-18**, 25 (1987).
³P. Hautojärvi, *Hyperfine Interact.* **15/16**, 357 (1983).
⁴Y. Yoshida, Ph.D. thesis, Osaka University, Japan, 1983.
⁵G. D. Sprouse, G. M. Kalvius, and S. S. Hanna, *Phys. Rev. Lett.* **18**, 1041 (1967).
⁶J. Christiansen, P. Hindenach, U. Morfeld, D. Riegel, E. Recknagel, and G. Weyer, *Nucl. Phys.* **A99**, 345 (1967).
⁷E. Recknagel, in *Nuclear Spectroscopy and Reactions, Part C*, edited by C. J. Czerny (Academic, New York, 1974), p. 93.
⁸E. Dafni, J. W. Noé, M. H. Rafailovich, and G. D. Sprouse, *Phys. Lett.* **76B**, 51 (1978); S. Vajda, G. D. Sprouse, M. H. Rafailovich, and J. W. Noé, *Phys. Rev. Lett.* **47**, 1230 (1981); M. H. Rafailovich, E. Dafni, J. M. Brennan, and G. D. Sprouse, *Phys. Rev. C* **27**, 602 (1983).
⁹R. S. Raghavan and P. Raghavan, *Nucl. Instrum. Methods* **92**, 435 (1971).
¹⁰C. E. Violet and D. N. Pipkorn, *J. Appl. Phys.* **42**, 4339 (1971).
¹¹M. Devillers, J. Ladriere, and D. Apers, *Hyperfine Interact.* **30**, 205 (1986).
¹²M. Menningen, Ph.D. thesis, Freie Universität Berlin, Berlin, West Germany, 1982.
¹³M. Kiritani, in *Proceedings of the 5th Yamada Conference on Point Defects and Defect Interactions in Metals*, edited by J. I. Takamura, M. Doyama, and M. Kiritani (Univ. of Tokyo Press, Tokyo, 1981), p. 59.
¹⁴D. G. Doran, *Radiat. Eff.* **2**, 249 (1970).
¹⁵A. Seeger, in *Radiation Damage in Solids* (IAEA, Vienna, 1962), p. 101.
¹⁶M. Menningen, H. Haas, H. H. Bertschat, R. Butt, H. Grawe, R. Keitel, R. Sielemann, and W.-D. Zeitz, *Phys. Lett.* **77A**, 455 (1980).
¹⁷H. Bertschat, H. Haas, F. Pleiter, E. Recknagel, E. Schlotter, and B. Spellmeyer, *Phys. Rev. B* **12**, 1 (1975); R. Butt, H. Haas, T. Butz, W. Mansel, and A. Vasquez, *Phys. Lett.* **64A**, 309 (1977).
¹⁸M. H. Rafailovich, E. Dafni, H.-E. Mahnke, G. D. Sprouse, and E. Vapirev, *Hyperfine Interact.* **10**, 821 (1981).
¹⁹M. B. Stearns, *Phys. Rev.* **147**, 439 (1966).
²⁰F. van der Woude and G. A. Sawatzky, *Phys. Rep.* **12**, 335 (1974).
²¹J. Korecki and U. Gradmann, *Phys. Rev. Lett.* **55**, 2491 (1985).
²²W. Mansel, J. Marangos, and D. Wahl, *J. Nucl. Mater.* **108/109**, 137 (1982).